

## Helical Rosette Nanotubes: Design, Self-Assembly, and Characterization

Hicham Fenniri,\* Packiarajan Mathivanan, Kenrick L. Vidale, Debra M. Sherman,† Klaas Hallenga,‡ Karl V. Wood,§ and Joseph G. Stowell||

1393 H. C. Brown Chemistry Laboratory  
Purdue University West Lafayette, Indiana 47907-1393

Received December 14, 2000

Organic,<sup>1</sup> inorganic,<sup>2</sup> and surfactant-derived<sup>3</sup> discrete tubular architectures have been the subject of intense investigation in the fields of materials science, nanotechnology, molecular electronic and photonic devices, sensor and artificial channel systems. Here we present evidence in support of a *modus operandi* for the hierarchical self-assembly of organic nanotubes from self-assembled supermacrocycles (rosettes)<sup>3f,g,4</sup> of low-molecular weight synthetic modules, under physiological conditions.

For a system based on hydrogen bonds to self-assemble in water one has to balance the enthalpic loss (H-bonds) with a consequent entropic gain (stacking interactions and hydrophobic effect). If preorganized, ionic H-bonds could also add to the enthalpic term. Nature has ingeniously taken advantage of these design principles to compartmentalize the cell (membranes), and to create thermodynamically favorable pathways for protein and nucleic acids folding. With this in mind, self-assembling L-module 1 (Figure 1a) was designed and synthesized with the following features: (a) a hydrophobic base unit possessing the Watson–Crick donor–donor–acceptor (DDA) H-bond array of guanine and acceptor–acceptor–donor (AAD) of cytosine. The spatial arrangement of these arrays constrains **1** to form a six-membered supermacrocycle (rosette, Figure 1b),<sup>4a,b</sup> (b) A methyl group (<sup>3</sup>HNCH<sub>3</sub>) was introduced to minimize peripheral access of water and to enforce the formation of an intramolecular ionic hydrogen bond between the side chain secondary ammonium and the neighboring ring carbonyl. (c) An ethylene spacer unit linking the base component to the chiral center was chosen to allow for said intramolecular

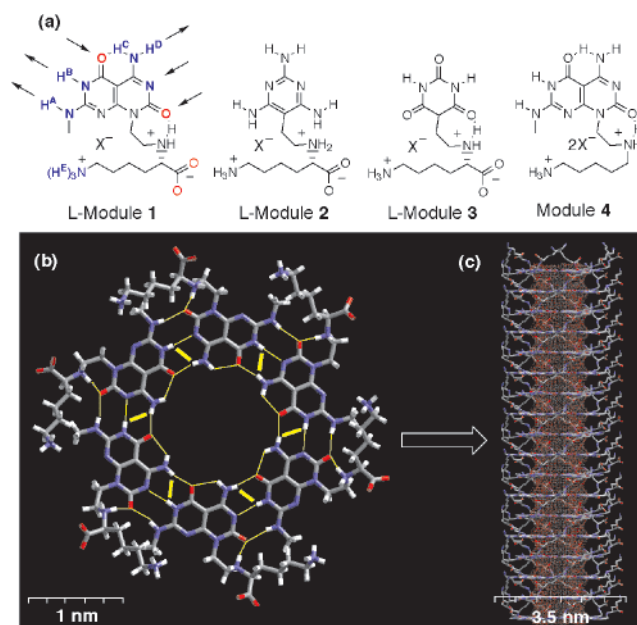


**Figure 1.** Hierarchical self-assembly of rosette nanotubes from L-module 1. (a) Modules 1–4 synthesized and investigated. (b) Molecular model of the rosette structure resulting from **1**. The thin yellow lines show the hydrogen-bond network. The thick yellow lines highlight unique intermolecular NOEs recorded. (c) Molecular model of the proposed nanotube. Eighteen rosettes were arranged in a tubular fashion with a starting interplane distance of 4.5 Å and 30° rotation along the tube's main axis.<sup>6</sup> The inner solvent-accessible surface area of the tube is highlighted in red.

ionic H-bond. (d) An amino acid moiety that dictates the supramolecular chirality of the resulting assembly was chosen. This tri-block design endows **1** with elements essential for the sequential self-assembly into stable nanotubular architectures (Figure 1c). Although a few natural<sup>5</sup> and synthetic<sup>3f,g,4</sup> compounds were shown to form supermacrocyclic assemblies in organic solvents, and in solid and liquid crystalline states, none are known to self-assemble into supermacrocycles or discrete nanotubular assemblies in water.

A synthetic scheme was devised to allow for oligomerization and functionalization at virtually any position of **1**.<sup>6</sup> **2**–**4** were prepared to establish the role of the stacking interactions, hydrophobic effect, and the chirality of the side chain in the assembly of the tubular architectures.

fb-NOESY <sup>1</sup>H NMR (600 MHz) in 90% H<sub>2</sub>O/D<sub>2</sub>O of **1** displayed nuclear Overhauser effects (NOEs) not only between H<sup>A</sup> and H<sup>B</sup> but also between H<sup>B</sup> and H<sup>C</sup>/H<sup>D</sup>.<sup>6</sup> Since H<sup>B</sup> and H<sup>C</sup>/H<sup>D</sup> are too far apart to display any *intra*-modular NOEs, the observation of an NOE between them confirms the existence of *inter*-modular H-bonds as highlighted in Figure 1b. This result is also diagnostic of the formation of the rosette structure since no other NOEs or imino proton signals resulting from nonassembled **1** or nonspecific aggregates thereof were observed. In agreement with this, electrospray ionization mass spectrometry (ESI-MS) of dilute aqueous solutions of **1** displayed all the peaks corresponding to the noncovalent intermediate species (1-mer to 6-mer) of the parent rosette.<sup>6</sup> Under the same conditions an equimolar aqueous mixture of the complementary, rosette forming, **2** and **3** did not undergo self-assembly (data not shown).

(5) (a) G. Gottarelli; Mezzina, E.; Spada, G. P.; Carsughi, F.; Di Nicola, G.; Mariani, P.; Sabatucci, A.; Bonazzi, S. *Helv. Chim. Acta* **1996**, *79*, 220–234. (b) Forman, S. L.; Fetting, J. C.; Pieraccini, S.; Gotarelli, G.; Davis, J. T. *J. Am. Chem. Soc.* **2000**, *122*, 4060–4067. (c) Marsh, T. C.; Vesenska, J.; Henderson, E. *Nucleic Acids. Res.* **1995**, *23*, 696–700.

(6) See Supporting Information.

\* Electron Microscopy Facility-Agriculture, Purdue University.

† NMR Center, Purdue University.

‡ Mass Spectrometry Center, Purdue University.

§ School of Pharmacy, Purdue University.

(1) (a) Harada, A.; Li, J.; Kamachi, M. *Nature* **1993**, *364*, 516–518. (b) Nelson, J. C.; Saven, J. G.; Moore, J. S.; Wolyne, P. G. *Science* **1997**, *277*, 1793–1796. (c) Ashton, P. R.; Brown, C. L.; Menzer, S.; Nepogodiev, S. A.; Stoddart, J. F.; Williams, D. J. *Chem. Eur. J.* **1996**, *2*, 580–591. (d) Ghadiri, M. R.; Granja, J. R.; Milligan, R. A.; McRee, D. E.; Kazanovich, N. *Nature* **1993**, *366*, 324–327. (e) Roks, M. F. M.; Nolte, R. J. M. *Macromolecules* **1992**, *25*, 5398–5407.

(2) (a) Iijima, S. *Nature* **1991**, *354*, 56–58. (b) Hamilton, E. J. M.; Dolan, S. E.; Mann, C. M.; Colijin, H. O.; McDonald, C. A.; Shore, S. G. *Science* **1993**, *260*, 659–661. (c) Brumlik, C. J.; Martin, C. R. *J. Am. Chem. Soc.* **1991**, *113*, 3174–3175. (d) Shenton, W.; Douglas, T.; Young, M.; Stubbs, G.; Mann, S. *Adv. Mater.* **1999**, *11*, 253–256. (e) Chopra, N. G.; Luyken, R. J.; Cherrey, K.; Crespi, V. H.; Cohen, M. L.; Louie, S. G.; Zettl, A. *Science* **1995**, *269*, 966–967.

(3) (a) Schnur, J. M. *Science* **1993**, *262*, 1669–1676. (b) Nakashima, N.; Asakuma, S.; Kunitake, T. *J. Am. Chem. Soc.* **1985**, *107*, 509–510. (c) Fuhrhop, J.-H.; Spiroski, D.; Boettcher, C. *J. Am. Chem. Soc.* **1993**, *115*, 1600–1601. (d) Frankel, D. A.; O'Brien, D. F. *J. Am. Chem. Soc.* **1994**, *116*, 10057–10069. (e) Imae, T.; Takahashi, Y.; Maramatsu, H. *J. Am. Chem. Soc.* **1992**, *114*, 3414–3419. (f) Kimizuka, N.; Fujikawa, S.; Kuwahara, S.; Kunitake, T.; Marsh, A.; Lehn, J.-M. *Chem. Commun.* **1995**, 2103–2104. (g) Klok, H.-A.; Joliffe, K. A.; Schauer, C. L.; Prins, L. J.; Spatz, J. P.; Möller, M.; Timmerman, P.; Reinhoudt, D. N. *J. Am. Chem. Soc.* **1999**, *121*, 7154–7155.

(4) (a) Mascal, M.; Hext, N. M.; Warmuth, R.; Moore, M. H.; Turkenburg, J. P. *Angew. Chem., Int. Ed. Engl.* **1996**, *35*, 2204–2206. (b) Marsh, A.; Silvestri, M.; Lehn, J.-M. *Chem. Commun.* **1996**, 1527–1528. (c) Whitesides, G. M.; Simanek, E. E.; Mathias, J. P.; Seto, C. T.; Chin, D. N.; Mammen, M.; Gordon, D. M. *Acc. Chem. Res.* **1995**, *28*, 37–44. (d) Kolotuchin, S. V.; Zimmerman, S. C. *J. Am. Chem. Soc.* **1998**, *120*, 9092–9094. (e) Meléndez, R. E.; Hamilton, A. D. *Top. Curr. Chem.* **1998**, *198*, 97–129.

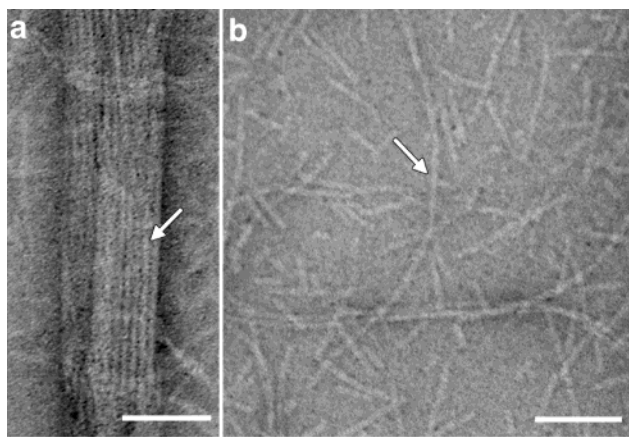


**Figure 2.** Transmission electron microscopy (TEM) of the rosette nanotubes obtained from the hierarchical self-assembly of **1**. The arrows point at individual nanotubes with  $\sim 4.0$  nm outer diameter. (a) TEM image of a nanotube bundle (b) TEM image representing the majority of the sample ( $\sim 90\%$ ). Scale bar = 50 nm.

Correlation between the supramolecular chirality of folate-<sup>5a</sup> and G-quadruplexes<sup>5b,c</sup> and circular dichroism (CD) activity has been drawn on the basis of exciton coupling theory.<sup>7</sup> The signed order of the CD exciton couplet is governed by the relative helicity of the relevant two electric dipole transition moments, one from each stacked base. The CD spectra of **1** and its D-isomer in an aqueous buffered solution display a typical couplet centered at 286 nm, characteristic of stacked bases in a helical environment, that vanishes at higher temperatures.<sup>1b,5,6,8</sup> Under identical conditions, **2** and **3** or an equimolar mixture of both, as well as the achiral **4** were CD-silent (data not shown).

The hyperchromicity observed upon deoxyribonucleic acids (DNA) denaturation is a powerful indicator of its stability and tertiary structure.<sup>9</sup> In this regard, the supramolecular outcome of **1** behaves very much like DNA: The absorbance spectrum undergoes a cooperative hyperchromic effect as the temperature increases (melting temperature  $T_m^{285\text{nm}} = 50$  °C). The same transition was recorded by variable temperature CD ( $\lambda = 292$  nm).<sup>6</sup> In combination with NMR, ESI-MS, and CD it became clear that: (a) **1** undergoes a cooperative, hierarchical self-assembly process through H-bonding, stacking interactions, and hydrophobic effects. (b) The assembly generated displays supramolecular chirality, most likely the result of helically stacked rosettes.

To assess the size of the assemblies generated, the dynamic light-scattering (DLS) spectrum was recorded for a buffered solution of **1**.<sup>6</sup> The narrow distribution (92% in the range 19–69 nm) obtained with an average apparent hydrodynamic radius,  $R_H$ , of 30.4 nm was rationalized by invoking a columnar stack reminiscent of the solid or liquid crystalline states of folate-<sup>5a</sup> and G-quadruplexes,<sup>5b,c</sup> and other self-assembled materials.<sup>3f,g,10</sup> As control experiments, **2**, **3**, or an equimolar mixture of both did not generate any detectable aggregate (data not shown).

(7) Nakanishi, K.; Berova, N. In *Circular Dichroism, Principles and Applications*; Nakanishi, K., Berova, N., Woody, R. W., Eds.; Wiley: VCH: New York, 1994; Chapter 13.

(8) Lahiri, S.; Thompson, J. L.; Moore, J. S. *J. Am. Chem. Soc.* **2000**, *122*, 11315–11319.

(9) Cantor, C. R.; Schimmel, P. R. *Biophysical Chemistry*; Freeman: New York, 1980.

(10) Hirschberg, J. H. K. K.; Brunsveld, L.; Ramzi, A.; Vekemans, J. A. J. M.; Sijbesma, R. P.; Meijer, E. W. *Nature* **2000**, *407*, 167–170.

TEM provided us with a visual evidence of the formation of the proposed nanotubular assemblies and a confirmation of the spectroscopic data discussed above. Figure 2 is a negatively stained sample of the nanotubes derived from **1** showing that: (a) all of the assemblies have the same outer hydrodynamic diameter ( $\sim 4.0$  nm), in agreement with the computed one. (b) In agreement with the DLS data, the length of over 90% of the nanotubular assemblies revolves around 60 nm. (c) Although  $\sim 10\%$  of the sample forms bundles (Figure 2a), there are no higher-order twisted or helical aggregates, thereby suggesting that the CD spectra recorded are the result of an intrinsic property of each individual nanotube.

At this point, we do not have direct visual evidence for the proposed rosette-stacking mode. However, the following additional observations led us to believe in its prevalence: (a) The simplicity of the <sup>1</sup>H NMR spectrum is indicative of a highly symmetrical assembly. A multihelical aggregate would create a dissymmetry in the H-bonding network, and as a result, multiple sets of protons would be recorded by NMR spectroscopy. (b) MS and NMR data support the formation of the basic component of the nanotubes, the rosette assembly. (c) The inoccurrence of branched and higher-order twisted aggregates by TEM precludes the possibilities for multistranded helical assemblies. (d) The remarkable consistence between the calculated rosette- and observed nanotube-diameter and its constancy throughout the entire sample support the proposed stacking mode. We also anticipate that *inter*-rosette ionic bridges between carboxylates and ammoniums lead to the formation of a six-stranded helicoidal electrostatic belt that contributes to the stabilization of the final assembly. Work to establish the role of these secondary interactions is currently underway.

This system establishes that electrostatic, stacking, and hydrophobic interactions can be effectively orchestrated by hydrogen bonds to direct the hierarchical assembly and organization of helical nanotubular architectures in an aqueous milieu. Understanding and exploring the electronic and structural elements that contribute to the formation of these assemblies may open new avenues for the design of nanoscale materials with predefined dimensions, shape, and function. Indeed, how would the pH, ionic strength, or solvents affect the hierarchical assembly? What would be the effect of amino acids, peptides, or other side chains on the supramolecular outcome? Could the tubular assemblies be further organized into nanoporous solid and liquid crystalline materials? The amenability of the synthetic scheme<sup>6</sup> to oligomerization and incorporation of alternative chiral components and bases (mono-, bi-, and tricyclic systems) will not only allow us to address these questions but will also provide us with a rapid access to tubular assemblies with predefined dimensions, photonic, electronic, and transport properties.

**Acknowledgment.** H.F. dedicates this work to Richard A. Lerner. We acknowledge the support of the National Science Foundation (Career award), the American Cancer Society (ACS-IRG 58), the American Chemical Society (ACS-PRF), the Showalter Foundation, and Purdue University. H.F. is a Cottrell Scholar of Research Corporation.

**Supporting Information Available:** Synthetic schemes for **1–4**; fb-NOESY, ESI-MS, UV-vis, CD, UV-vis melting curve, DLS, TEM, and molecular models of the rosette nanotubes resulting from **1** (PDF). This material is available free of charge via the Internet at <http://pubs.acs.org>.

JA005886L